

The impact of UV photons from a stellar companion on the chemistry of AGB outflows

M. Van de Sande^{1,2}  and T. J. Millar³

¹School of Physics and Astronomy, University of Leeds, Leeds LS2 9JT, UK
email: m.vandesande@leeds.ac.uk

²Institute of Astronomy, KU Leuven, Celestijnenlaan 200D, 3001 Leuven, Belgium

³Astrophysics Research Centre, School of Mathematics and Physics, Queen's University Belfast, University Road, Belfast BT7 1NN, UK
email: tom.millar@qub.ac.uk

Abstract. Binary interaction with a stellar or planetary companion has been proposed to be the driving mechanism behind large-scale asymmetries, such as spirals and disks, observed within AGB outflows. We developed the first chemical kinetics model that takes the effect of a stellar companions's UV radiation into account. The presence of a stellar companion can initiate a rich photochemistry in the inner wind. Its impact is determined by the intensity of the UV radiation and the extinction the radiation experiences. The outcome of the inner wind photochemistry depends on the balance between two-body reactions and photoreactions. If photoreactions dominate, the outflow can appear molecule-poor. If two-body reactions dominate, chemical complexity within the outflow can increase, yielding daughter species with a large inner wind abundance. A comprehensive view on the molecular content of the outflow, especially combined with abundance profiles, can point towards the presence of a stellar companion.

Keywords. Stars: AGB and post-AGB, circumstellar matter, astrochemistry, molecular processes

1. Introduction

Spherical asymmetry is prevalent within AGB outflows. Both small-scale asymmetries, such as density-enhanced clumps (e.g., [Leão *et al.* \(2006\)](#); [Khouri *et al.* \(2016\)](#); [Agúndez *et al.* \(2017\)](#)), and large-scale structures, such as spirals (e.g., [Mauron & Huggins \(2006\)](#); [Maercker *et al.* \(2016\)](#)) and disks (e.g., [Kervella *et al.* \(2014\)](#); [Homan *et al.* \(2018\)](#)), have been widely observed. These asymmetries are thought to be induced by binary interaction with a stellar or planetary companion (e.g., [Decin *et al.* \(2015\)](#); [Ramstedt *et al.* \(2017\)](#); [Moe & Di Stefano \(2017\)](#); [Decin *et al.* \(2020\)](#)). A stellar companion will radiate part of its energy in the ultraviolet (UV). These photons may disrupt the chemistry throughout the outflow, potentially allowing molecular abundances to be a tool to distinguish between a stellar and planetary companion.

We developed the first chemical kinetics model that takes the effect of UV radiation from a nearby stellar companion into account. Our one-dimensional model is a first approximation of the effects on the chemistry within an AGB outflow, paving the way for future model development. In Sect. 2, we summarise the main characteristics and limitations of the model. Highlights of our results are given in Sect. 3, followed by our

Table 1. Physical parameters of the grid of chemical models.

Density structures	Smooth outflow Two-component clumpy outflow $f_{ic} = 0.3, f_{vol} = 0.3, l_* = 4 \times 10^{12}$ cm One-component clumpy outflow $f_{ic} = 0.0, f_{vol} = 0.3, l_* = 4 \times 10^{12}$ cm
Outflow density, $\dot{M} - v_\infty$	$10^{-5} M_\odot \text{ yr}^{-1} - 15 \text{ km s}^{-1}$ $10^{-6} M_\odot \text{ yr}^{-1} - 5 \text{ km s}^{-1}$ $10^{-7} M_\odot \text{ yr}^{-1} - 5 \text{ km s}^{-1}$
Stellar radius, R_*	2×10^{13} cm
Stellar temperature, T_*	2330 K
Exponent temperature power-law $T(r), \epsilon$	0.7
Onset of dust extinction, R_{dust}	2, 5 R_*
Companion temperature, T_{comp} , and radius, R_{comp} ,	4000 K - 1.53×10^{10} cm 6000 K - 8.14×10^{10} cm 10 000 K - 6.96×10^8 cm
Inner radius of the model	$1.025 \times R_{dust}$

conclusions in Sect. 4. A full description of the model and all our results can be found in [Van de Sande & Millar \(2022\)](#).

2. Chemical model

2.1. Physics

The physical parameters of the model are listed in Table 1. The chemical model is an extension of [Van de Sande & Millar \(2019\)](#), where we included the effect of stellar UV photons. Internal photons, i.e. stellar and companion photons, are extinguished by dust as well as geometrically diluted. The visual extinction experienced by internal photons depends on the onset of dust extinction, R_{dust} . Since the gas-phase model does not treat dust formation, dust is assumed to be present throughout the model. To simulate different dust condensation radii, we choose $R_{dust} = 2$ and $5 R_*$.

To include the effects of an inhomogeneous outflow in our one-dimensional model, we use the porosity formalism ([Van de Sande et al. \(2018\)](#)). The outflow is divided into a stochastic two-component medium, composed of overdense clumps and a tenuous interclump region. The clumpiness of the outflow is set by three parameters: the interclump density contrast, f_{ic} , the clump volume filling factor, f_{vol} , and the clump's size at the stellar surface, l_* . Besides a smooth outflow, we consider a two-component outflow and a one-component outflow (void interclump). These three density structures allow us to probe different behaviours of extinction experienced by interstellar and internal photons.

2.2. Chemistry

The parent species and their initial abundances for the O-rich and C-rich outflows are based on observations. They are taken from [Agúndez et al. \(2020\)](#), who compiled (ranges of) observed abundances in the inner regions of AGB outflows.

The stellar companion's UV flux is approximated by blackbody radiation. We vary over three types of companion, characterised by their blackbody temperature, T_{comp} , and radius, R_{comp} : a red dwarf ($T_{comp} = 4000$ K, $R_{dust} = 1.53 \times 10^{10}$ cm), a solar-like star ($T_{comp} = 6000$ K, $R_{dust} = 8.14 \times 10^{10}$ cm), and a white dwarf ($T_{comp} = 10\,000$ K and $R_{dust} = 6.96 \times 10^8$ cm). Cross sections are used to calculate the unshielded photodissociation and photoionisation rates. These are mainly taken from the Leiden Observatory

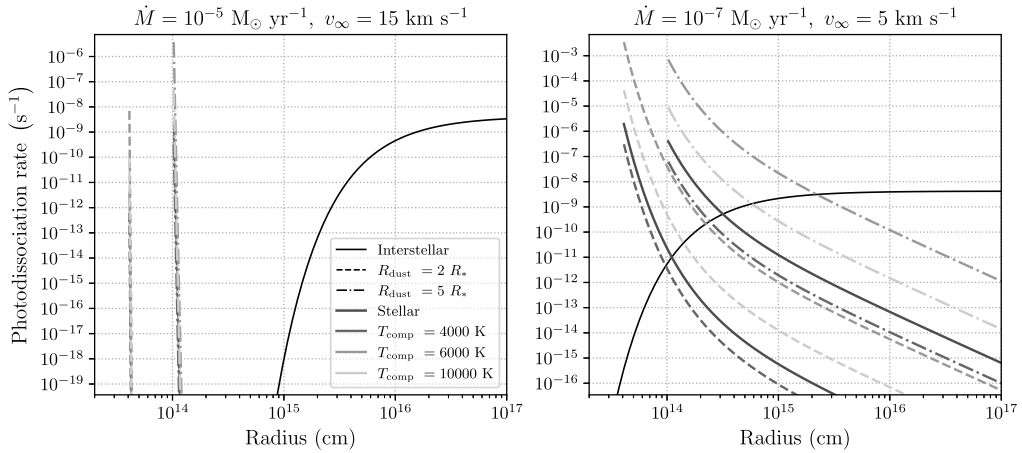


Figure 1. Photodissociation rates of SO in different outflow densities (left: highest outflow density, right: lowest outflow density). Black solid line: rate caused by interstellar UV photons. Different shades of grey show the rate caused by stellar or companion UV photons. From darkest to lightest: stellar UV photons ($T_* = 2330$ K), red dwarf companion UV photons, solar-like companion UV photons, white dwarf companion UV photons. Different line styles show the location of the onset of dust extinction. Dashed: $R_{\text{dust}} = 2 R_*$, dotted: $R_{\text{dust}} = 5 R_*$.

Database (Heays *et al.* (2017))†. If cross section are not available, the rate coefficients are estimated by scaling the unshielded interstellar rate by the ratio of the integrated fluxes of companion photons to interstellar photons over the 912 – 2150 Å range. This scaling, which is often used in astrochemistry, can lead to large errors, particularly for photoionisation rates at low black body temperatures. The specific scalings adopted for $T_{\text{comp}} = 4000$ and 6000 K can be found in Van de Sande & Millar (2022).

Figure 1 shows the photodissociation rate of SO in a high density and low density smooth outflow, caused by interstellar, stellar and companion UV outflows and varying over R_{dust} . The onset of photodissociation is set by the outflow density and R_{dust} , as they determine the extinction experienced. The rate is determined by the intensity of the companion’s radiation, set by T_{comp} and R_{comp} . A solar-like companion yields the largest photodissociation rates; a red dwarf yields photodissociation rates comparable to those of stellar photons.

2.3. Limitations

Several assumptions go into our model. Since we build on our previous work, the companion is assumed to be located at the centre of the AGB star. While unrealistic, the effects of misplacing the companion within $5 R_*$ (the largest value of R_{dust}) is negligible compared to the scale of the outflow. Additionally, because the model is one-dimensional, orbital effects cannot be taken into account. The underlying assumption of a continuously radiating companion is relatively reasonable for close-by companions, considering the limited fraction of the entire outflow that experiences occultation of the companion by the AGB star: gas at $10 R_*$ will see the UV field of a companion orbiting at $2 R_*$ for 80% of its orbital period. For more details, we refer to Van de Sande & Millar (2022).

3. Results

The presence of a stellar companion can initiate a rich photochemistry in the dense inner wind, photodissociating and photoionising parents. This type of chemistry is typical

† <https://home.strw.leidenuniv.nl/~ewine/photo/>

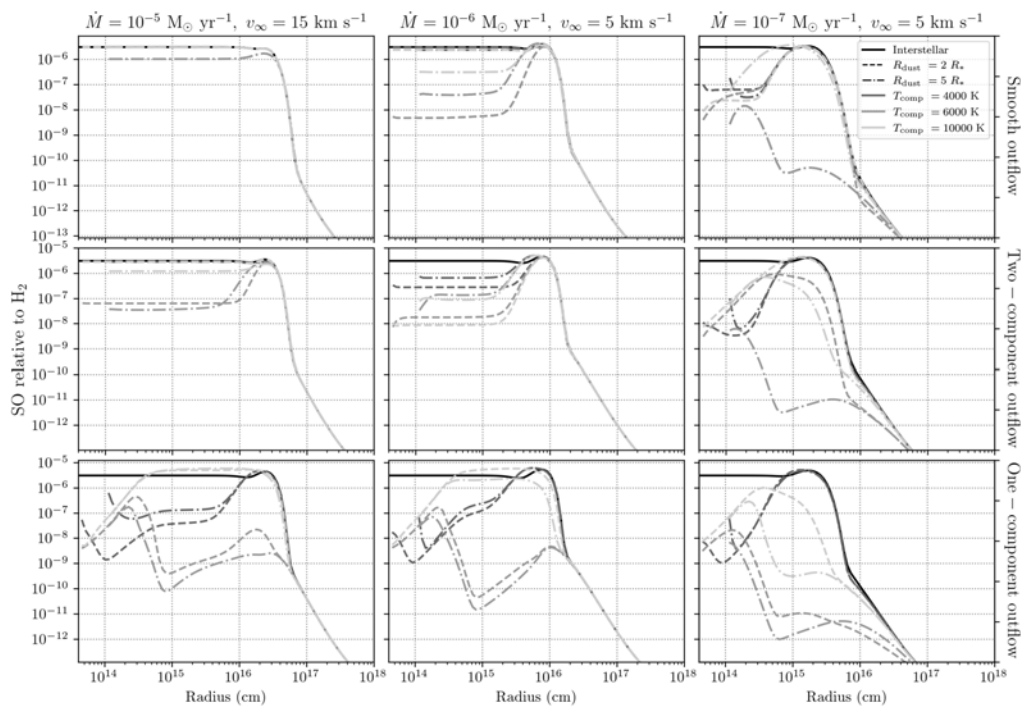


Figure 2. Fractional abundance of SO in O-rich outflows with different outflow densities (columns) and density structures (rows). Black, solid lines: results including interstellar photons only. Different shades of grey show the results included stellar and companion photons. From darkest to lightest: red dwarf companion UV photons, solar-like companion UV photons, white dwarf companion UV photons. Different line styles show the location of the onset of dust extinction. Dashed: $R_{\text{dust}} = 2 R_*$, dotted: $R_{\text{dust}} = 5 R_*$.

for the outer, tenuous regions of the outflow. The outcome of the inner wind photochemistry and its effects on the chemistry throughout the entire outflow depend mainly on the extinction experienced by internal photons (set by the outflow density and structure), as well as on the intensity of the companion's UV radiation (set by T_{comp} and R_{comp}).

As the outflow density decreases and/or the outflow becomes more porous, the amount of UV radiation throughout the outflow increases. The extinction in the smooth outflow with $\dot{M} = 10^{-5} M_{\odot} \text{ yr}^{-1}$ is too large for internal photons to have any impact. We can distinguish between high UV outflows, where internal photons experience little extinction, and low UV outflows, where they experience moderate amount of extinction. High UV outflows have a low outflow density and/or are highly porous. In our grid, these are the one-component outflow with $\dot{M} = 10^{-6} M_{\odot} \text{ yr}^{-1}$ and all outflows with $\dot{M} = 10^{-7} M_{\odot} \text{ yr}^{-1}$. In these outflows, two-body reactions are slower than photoreactions. This inhibits reformation of newly photodissociated parent species and any subsequent reactions between daughter species, reducing the outflow to an apparently molecule-poor state. Consequently, low UV outflows have a higher outflow density and/or a lower porosity. These are all porous outflows with $\dot{M} = 10^{-5} M_{\odot} \text{ yr}^{-1}$ and the smooth and two-component outflow with $\dot{M} = 10^{-6} M_{\odot} \text{ yr}^{-1}$. In these outflows, two-body reactions are faster than photoreactions. Chemical complexity increases, as newly formed daughter species can readily react before further photoreactions. Species that are otherwise produced in the outer regions can now be abundantly present in the inner wind. This can result in abundance profiles similar to those of parent species, with a large inner wind abundance followed by a gaussian decline. A red dwarf companion does not significantly

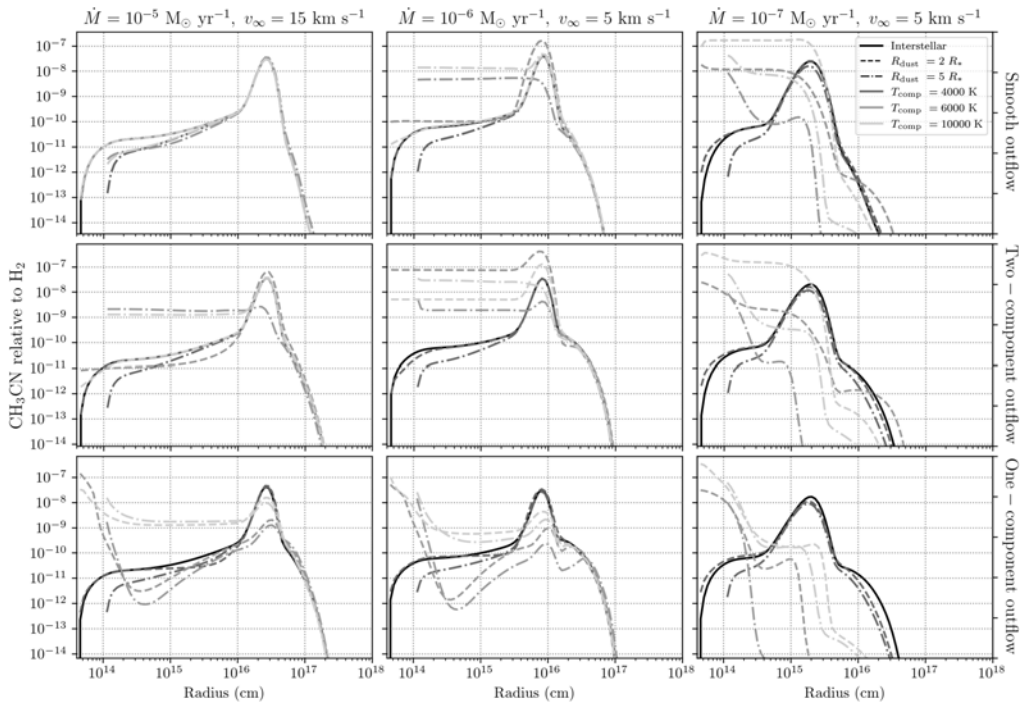


Figure 3. Fractional abundance of CH_3CN in C-rich outflows with different outflow densities (columns) and density structures (rows). Black, solid lines: results including interstellar photons only. Different shades of grey show the results included stellar and companion photons. From darkest to lightest: red dwarf companion UV photons, solar-like companion UV photons, white dwarf companion UV photons. Different line styles show the location of the onset of dust extinction. Dashed: $R_{\text{dust}} = 2 R_*$, dotted: $R_{\text{dust}} = 5 R_*$.

influence the chemistry, except in outflows with low outflow density and a porous structure. A solar-like companion shows the largest impact. Despite the larger temperature of the white dwarf companion, its compact size reduces the impact on the photochemistry.

Figure 2 shows the abundance of the parent SO in O-rich outflows. In most low UV outflows, the initial abundance of SO appears to be reduced by up to three orders of magnitude, followed by an increase in its abundance forming a bump. The bump is caused by reformation of SO via $\text{S} + \text{OH}$, two photodissociation products. This type of profile has been observed around higher mass-loss rate O-rich AGB stars (Danilovich *et al.* (2016, 2020)). In high UV outflows with a bright solar-like or white dwarf companion, as well as the low UV one-component outflow with $\dot{M} = 10^{-5} M_{\odot} \text{ yr}^{-1}$ and a solar-like companion, OH itself is photodissociated, reducing or eliminating the bump and rendering the outflow apparently poor in SO.

Figure 3 shows the abundance of the daughter CH_3CN in C-rich outflows. In low UV outflows, CH_3CN is formed in the innermost regions via the reaction $\text{HCN} + \text{CH}_3^+$, followed by dissociative recombination with an electron. This reaction channel highlights the delicate balance between two-body reactions and photoreactions: enough UV radiation is necessary to produce CH_3^+ , a second-generation daughter of the parent CH_4 , while the parent HCN should still be abundantly present. The resulting parent-like abundance profile (large initial abundance followed by a gaussian decline) has been observed around IRC+10216 (Agúndez *et al.* (2015)). In high UV outflows, any newly formed CH_3CN is rapidly photodestroyed.

4. Conclusions

Stellar companions can initiate a rich photochemistry in the inner regions of the outflow. The effects on the chemistry throughout the outflow depend mainly on the outflow density and structure, as well as on the companion's UV radiation field. The resulting chemistry is determined by the balance between two-body reactions and photoreactions. In outflows where internal photons experience an intermediate amount of dust extinction and where mass-loss rates are higher, two-body reactions are faster than photoreactions. This can increase the chemical complexity of the outflow, with daughter species showing a parent-like abundance profile of a large inner abundance followed by a gaussian decline. In outflows where internal photons experience little dust extinction, photoreactions are faster. Parents and newly formed daughters can be rapidly photodissociated, rendering the outflow apparently molecule-poor.

Our chemical model is the first to take any effects of a stellar companion on the chemistry throughout an AGB outflow into account. We find that the resulting chemistry is highly dependent on the outflow's density and structure, the type of stellar companion, as well as the assumed parent species and their initial abundances. Nonetheless, our simplified model shows that the chemical composition of the outflow can be used as a tool to distinguish between a stellar and substellar companion, and paves the way for further (three-dimensional) model development.

Acknowledgements

MVdS acknowledges support from the Research Foundation Flanders (FWO) through grant 12X6419N and the European Union's Horizon 2020 research and innovation programme under the Marie Skłodowska-Curie grant agreement No 882991. TJM gratefully acknowledges the receipt of a Leverhulme Emeritus Fellowship and the STFC for support under grant reference ST/P000312/1 and ST/T000198/1.

References

- Agúndez, M., Cernicharo, J., Quintana-Lacaci, G. *et al.* 2015, *ApJ*, 814, 143
Agúndez, M., Cernicharo, J., Quintana-Lacaci, G. *et al.* 2017, *A&A*, 601, A4
Agúndez, M., Martínez, J. I., de Andres, P. L. *et al.* 2020, *A&A*, 637, A59
Danilovich T., De Beck E., Black J. H. *et al.* 2016, *A&A*, 588, A119
Danilovich T., Richards A. M. S., Decin L. *et al.* 2020, *MNRAS*, 494, 1323
Decin L., Richards A. M. S., Neufeld D. *et al.* 2015, *A&A*, 574, A5
Decin, L., Montargès M., Richards, A. M. S. *et al.* 2020, *Science*, 369, 1497
Heays, A. N., Bosman, A. D. and van Dishoeck, E. F. 2017, *A&A*, 602, A105
Homan W., Danilovich T., Decin L. *et al.* 2018, *A&A*, 614, A113
Kervella, P., Montargès, M., Ridgway, S. T. *et al.* 2014, *A&A*, 564, A88
Khouri, T., Maercker, M., Waters, L. B. F. M. *et al.* 2016, *A&A*, 591, A70
Leão, I. C., de Laverny, P., Mékarnia, D. *et al.* 2006, *A&A*, 455, 187
Maercker M., Danilovich T., Olofsson H. *et al.* 2016, *A&A*, 591, A44
Mauron N. & Huggins P. J. 2006, *A&A*, 452, 257
Moe M. & Di Stefano R. 2017, *ApJS*, 230, 15
Ramstedt, S., Mohamed, S., Vlemmings, W. H. T. *et al.* 2017, *A&A*, 605, A126
Van de Sande, M., Sundqvist, J. O., Millar, T. J. *et al.* 2018, *A&A*, 616, A106
Van de Sande, M. & Millar, T. J. 2019, *ApJ*, 873, 36
Van de Sande, M. & Millar, T. J. 2022, *MNRAS*, 510, 1204